RICARDO ANDRADE PINTO JUNIOR

HIGH THROUGHPUT EAR PHENOTYPING: APLICATION IN SWEET CORN

LAVRAS – MG

2020

RICARDO ANDRADE PINTO JÚNIOR

HIGH THROUGHPUT EAR PHENOTYPING: APLICATION IN SWEET CORN

Tese apresentada à Universidade Federal de Lavras, como parte das exigências do Programa de Pós-Graduação em Genética e Melhoramento de Plantas, área de concentração Genética e Melhoramento de Plantas para obtenção do título de doutor.

Prof. Dr. Renzo Garcia Von Pinho
Orientador

LAVRAS – MG
2020

Ficha catalográfica elaborada pelo Sistema de Geração de Ficha Catalográfica da Biblioteca Universitária da UFLA, com dados informados pelo(a) próprio(a) autor(a).

Pinto Junior, Ricardo Andrade.
High Throughput Ear Phenotyping: Aplication In Sweet Corn / Ricardo Andrade Pinto Junior. - 2020.
49 p. : il.

Orientador(a): Renzo Garcia Von Pinho.

Tese (doutorado) - Universidade Federal de Lavras, 2020.
Bibliografia.

1. Milho doce. 2. Fenotipagem. 3. Melhoramento. I. Von Pinho, Renzo Garcia. II. Título.

RICARDO ANDRADE PINTO JÚNIOR

HIGH THROUGHPUT EAR PHENOTYPING: APLICATION IN SWEET CORN
FENOTIPAGEM DE ALTO RENDIMENTO EM ESPIGAS DE MILHO DOCE

Tese apresentada à Universidade Federal de Lavras, como parte das exigências do Programa de Pós-Graduação em Genética e Melhoramento de Plantas, área de concentração Genética e Melhoramento de Plantas para obtenção do título de doutor.

APROVADA em 29/10/2020

Dr. Renzo Garcia Von Pinho	UFLA
Dr. Marcio Fernando Ribeiro de Rezende Junior	UF-Florida
Dr. Vinícius Quintão Carneiro	UFLA
Dra. Flávia Maria Avelar Gonçalves	UFLA
Dr. Adriano Teodoro Bruzi	UFLA

Prof. Dr. Renzo Garcia Von Pinho
Orientador

LAVRAS – MG
2020

os meus pais, Ricardo e Luzia, a minha irmã Cristiane, e a minha noiva Francielly, que sempre me apoiaram e incentivaram nesta caminhada.

DEDICO!

AGRADECIMENTOS

Primeiramente agradeço à Deus por estar sempre presente e me guiando.

Aos meus pais, Ricardo e Luzia, e a minha irmã Cristiane pelo apoio, incentivo, aconselhamentos e companheirismo, amo vocês.

A minha noiva e futura esposa Francielly, pelo companheirismo e cumplicidade em todos os momentos decisivos, posso dizer que neste período o meu crescimento profissional e pessoal foi muito influenciado por ela, uma das pessoas mais incríveis que conheci em toda minha vida e tenho o privilegio de ser amado e amar essa mulher.

A todos os professores do programa de pós-graduação em Genética e Melhoramento de Plantas, pelos conhecimentos transmitidos e principalmente oportunidades recebidas, em especial ao professor Magno que além de referência intelectual, tenho como espelho em muitas das minhas atitudes e decisões, tanto profissionais como pessoais.

Aos amigos Emanuel, Thaise e Gustavo, que fizeram parte desta caminhada e como agradecimento pelo companheirismo deixo esta frase que ouvi certa vez “a única diferença entre os irmãos de sangue e os verdadeiros amigos é que os amigos você pode escolher”.

Ao professor e amigo Marcio Resende, por gentilmente ter cedido os dados para confecção desta tese, mas também pelas oportunidades oferecidas, uma das pessoas mais generosas que tive a oportunidade de conhecer.

Ao professor Renzo pela orientação e principalmente pelos valiosos conselhos.

Ao professor Marcio Balestre (in memoriam) pela coorientação.

À Universidade Federal de Lavras e ao Programa de Pós-Graduação em Genética e Melhoramento de Plantas pela oportunidade.

À Coordenação de Aperfeiçoamento de Pessoal de Nível Superior (CAPES) pela concessão de bolsa de estudos.

Para todos os colegas do Programa de Pós-Graduação em Genética e Melhoramento de Plantas e funcionários do departamento de biologia, que contribuíram de forma imprescindível para a minha vida acadêmica.

O presente trabalho foi realizado com apoio da Coordenação de Aperfeiçoamento de Pessoal de Nível Superior – Brasil (CAPES) – Código de Financiamento 001.

RESUMO

O uso de imagens na fenotipagem de alta precisão tem se mostrado uma técnica promissora para acelerar e aumentar os ganhos genéticos de caracteres qualitativos ligados a qualidade das espigas e a produtividade de grãos em programas de melhoramento de milho doce. Por isso, o objetivo desse estudo foi estabelecer um protocolo eficiente de fenotipagem de espigas, utilizando imagens digitais. A aquisição das imagens foi realizada em tempo reduzido em uma plataforma simples e de baixo custo. As imagens foram processadas em software gratuito utilizando técnicas de segmentação. Após o processamento das imagens, foram extraídas matrizes de píxeis que permitiram a caracterização das espigas quanto aos descritores comprimento, largura, área total, área sem preenchimento de grãos, número de fileira e número de grãos. Medidas de confiabilidade foram empregadas para verificar a eficiência da fenotipagem por meio das imagens digitais e sua concordância com a fenotipagem manual. As metodologias propostas se mostraram promissoras para caracterização das espigas de milho por meio das imagens. Foram observadas correlações elevadas, variando de 0,6 a 0,95, entre os valores estimados via imagens e os obtidos manualmente. As técnicas de segmentação de imagens e a metodologia proposta para determinar o comprimento e largura das espigas foi altamente eficiente. O uso de imagens reduziu o tempo e a mão de obra dispendidos na caracterização das espigas. O protocolo estabelecido nesse estudo pode substituir a fenotipagem manual e ser adotado em larga escala, sem custos elevados, em qualquer programa de melhoramento. Os resultados apresentados encorajam novas investigações ligadas ao processamento de imagens visando acelerar a fenotipagem de características de interesse do melhorista.

Palavras-chave: Fenotipagem. Imagens Digitais. Milho Doce

ABSTRACT

The use of digital images in high throughput phenotyping has been shown to be a promising technique to speed up and increase the genetic gains of qualitative traits linked to the quality of ears and grain productivity in breeding programs for sweet corn. Therefore, the goals of this study were to establish an efficient protocol for ear phenotyping, using digital images. The acquisition of the images was accomplished in a reduced time in a simple and low-cost platform. The images were processed in open software using image segmentation techniques. After processing the images, pixel matrices were extracted, which allowed the characterization of the ears in terms of length, width, total area, tip fill area, number of rows and number of kernels. Index of agreement were used to verify the efficiency of phenotyping through digital images when compared with manual phenotyping. The proposed methodologies were shown to be promising for the characterization of corn ears through digital images. High correlations were observed, ranging from 0.6 to 0.95, between the values estimated via images and those obtained manually. The techniques of image segmentation and the proposed methodology to determine the length and width of the ears were highly efficient. The use of images reduced the time and labor spent on characterizing the ears. The protocol established in this study can replace manual phenotyping and be adopted on a large scale, without high costs, in any breeding program. The results presented encourage further investigations related to image processing in order to speed up the phenotyping of characteristics of interest to the breeder.

Key-words: Phenotyping. Digital Images. Sweet Corn

LISTA DE FIGURAS

LISTA DE TABELAS

SUMÁRIO

1 INTRODUCTION

Consumption of fresh sweet corn (*Zea mays* var. rugosa) is very popular in the United States and Europe. Around the world, a large part of its production is destined for consumption processed in cans or frozen. Due to the market to which it is destined, sweet corn is classified as an olericulous crop and therefore, in addition to productivity it is important that the breeder is focused on qualitative aspects of the ears such as color, size, number of kernel rows, number of grains and area without grain filling, since the acceptance of ears by consumers is directly linked to their phenotypic quality (STEVENS et al., 2003).

Phenotyping sweet corn ears in breeding programs has been carried out over the years manually. Although it often involves simple processes, the characterization of many genotypes using traditional phenotyping methods, is considered an expensive process because it requires qualified labor, time, being a subjective and often destructive process (FURBANK; TESTER, 2011). Additionally, the collection of accurate phenotypic data has been considered one of the main bottlenecks in increasing genetic gain in breeding programs, especially when studies involve genomic information (DEERY et al., 2016; YANG et al., 2020).

Carrying out the phenotyping of corn ears accurately, quickly and efficiently is a major challenge for breeding programs, because characteristics directly related to grain yield such as length, width, number of rows and grains per ear, are activities costly and difficult to measure when many genotypes are being evaluated during the selection stages. Concomitantly, one must take into account the low precision associated with manual phenotyping due to the qualification discrepancy between the evaluators, calibration of the equipment used in the process and, above all, due to the physical and mental fatigue of the evaluators.

In the last decade, high-performance phenotyping has been identified as an alternative tool to accelerate the process and increase accuracy in identifying characteristics of interest to the breeder. The popularization, quality development and reduction in the cost of equipment such as cameras, drones, sensors and robotic platforms associated with the ease of storage and database processing, has doubled the number of works related to high-yield phenotyping in plants compared to other areas of research

such as genomics, proteomics and precision agriculture (COSTA et al, 2019; YANG et al., 2020).

Another factor that contributed to increase research on automated phenotyping was the evolution of studies in the field of genomics. While the use of molecular markers has become accessible for genotyping many individuals in breeding programs, the selective accuracy of the prediction models has been limited due to the difficulty and low precision in obtaining the phenotypic data that validate these models.

Ear phenotyping using images has been highlighted as an advantageous tool as it is a non-destructive, low-cost, easy-to-execute process highly correlated with information obtained manually. Studies show that automated phenotyping can replace manual ear phenotyping, improve the accuracy and speed of processing field data and assist the breeder in identifying characteristics of interest for the selection of superior genotypes (ZHAO et al, 2015; LIANG et al., 2016; MILLER et al., 2017; MAKANZA et al., 2018; WARMAN; Fowler, 2019).

Much of the work is using image segmentation algorithms to extract information. This technique has shown competitive results in efficacy and speed compared to manual phenotyping (ZHAO et al., 2015; MAKANZA et al., 2018; WARMAN; FOWLER, 2019). Associated with this, low-cost tools that enable phenotyping hundreds of ears and benefit breeding programs with limited resources, have been presented in the literature (MAKANZA et al., 2018; WARMAN; FOWLER, 2019; WU et al., 2020).

It is a fact that the use of digital images is an accurate, fast and low-cost option for phenotyping traits related to ears. However, most studies found in the literature use few ears, with low variability between them and with high phenotypic pattern, not reflecting the reality of many corn breeding programs. This fact associated with some crucial steps in the use of images for ear phenotyping, such as: background definition, processing, image segmentation and noise elimination, demonstrate that the best methodology for the characterization of ears is not yet well defined.

In this context, the goal of this study was to develop an efficient, fast, low-cost methodology, with high agreement with traditional protocols, to extract information related to the production and quality components of sweet corn ears, using digital images.

2 REFERENCIAL TEÓRICO

2.1 Fenotipagem por imagem

A fenotipagem consiste na determinação dos valores quantitativos ou qualitativos das características de um genótipo (DHONDT; WUYTS; INZE, 2013). A fenotipagem tradicional de plantas para os melhoristas inclui caminhar pelos campos experimentais e marcar parcelas com base na maioria das vezes na aparência das plantas. Melhorias nos métodos de fenotipagem são altamente desejáveis e devem adicionar equilíbrio entre precisão, acurácia, velocidade e custo. A fenotipagem de alto rendimento pode aumentar o que os melhoristas podem avaliar e oferecer melhores escolhas baseadas no fenótipo (ARAUS et al., 2018).

Neste contexto a possibilidade de fenotipagem de milhares de indivíduos, mais rápido e com alta precisão (DAVEY et al., 2011), essa tecnologia promete reduzir custos e agilizar o desenvolvimento de culturas mais bem adaptadas para os produtores em um ritmo mais rápido. As seleções baseadas em campo estão sujeitas a recursos e precisão limitados, mas ainda são altamente eficazes para caracterizar as respostas da cultura ao ambiente para muitas características que são mais complexas do que aquelas detectadas em um laboratório (KIM, 2020).

Uma série de componentes e etapas deve ser considerada para o desenvolvimento de um sistema de fenotipagem de alto rendimento, que inclui sensores, plataformas, análises e gerenciamento de dados (CRAIN et al., 2016).

O emprego de imagens digitais para fenotipagem pode trazer muitos benefícios. As técnicas para captura das imagens geralmente são rápidas, não invasivas, precisas, de baixo custo, livres de resíduos, com boa resolução espacial e temporal, permitem explorar áreas relativamente grandes, proporcionam grande número de repetições e segurança ao operador (SOUSA et al., 2015). A automação do processo de obtenção das imagens, dependendo da espécie vegetal, das condições de cultivo e das variáveis, viabiliza estudos comparativos e seleção fenotípica em larga-escala (GEBREMEDHIN et al., 2019). Por fim, a utilização dessas técnicas possibilita avaliar o impacto dos diferentes tipos de estresses sobre as plantas e parâmetros bioquímicos, sem a necessidade de destruí-las (SOUSA et al., 2015).

Há cinco tipos de sensores disponíveis para a captura de imagens em diferentes regiões do espectro eletromagnético: 1) sensores digitais para captura de imagens RGB; 2) sensores no visível para a captura de imagens de pigmentos; 3) sensores no infravermelho próximo para a captura de imagens relacionadas aos índices de água; 4) sensores no infravermelho longo para a captura de imagens térmicas; e 5) sensores para a captura de fluorescência, especialmente de clorofilas (ZHAO et al., 2019).

Esses sensores permitem o estudo de diversas características como: análise do crescimento; determinação de pigmentos, como clorofilas e carotenoides; avaliação do aparato fotoquímico; temperatura da copa, para identificação de estresse hídrico e salino (SOUSA et al., 2015, ZHAO et al, 2019). Apesar do potencial dessas ferramentas para fenotipagem em larga escala e vários trabalhos de fenotipagem em espigas de milho (VALIENTE-GONZÁLEZ et al., 2014; MILLER et al., 2017; MAKANZA et al., 2018; ZHAO et al., 2019; WU et al., 2020), nenhum trabalho realizou uma abordagem que utilizava software gratuito e proporcionasse os mesmo resultados com custo de execução e aplicação baixo.

2.3 Milho Doce

O milho doce (Zea mays L.), considerado uma olerícola, tem características particulares, como sabor doce, pericarpo fino e endosperma de textura delicada e alto valor nutritivo (KWIATKOWSKI; CLEMENTE, 2007). É destinado exclusivamente ao consumo humano, na forma in natura ou em alimentos processados, enquanto a palha pode ser utilizada para silagem após a colheita (TEIXEIRA et al., 2001).

A diferença entre o milho doce e o milho comum está no teor de açúcares e amido presentes no endosperma (ARAGÃO, 2002), resultantes da ação de genes recessivos individuais ou em associações. Assim, enquanto o milho comum tem em torno de 3% de açúcar e entre 60 e 70% de amido, o milho doce tem de 9 a 14% de açúcar e de 30 a 35% de amido (CAMILO, 2015).

Além do milho doce fresco para consumo humano, ele pode ser posteriormente processado em outros produtos alimentícios, adoçantes, amidos, óleos, álcool e combustível à base de etanol. O milho também é o principal grão de ração nos Estados Unidos e deve responder por cerca de 95% dos grãos de ração em 2015-2016. Em 2010,

os americanos consumiam em média 11.8 kg de milho doce por pessoa. Desse montante total, 4.3 kg eram de milho doce congelado, 4,1 kg eram milho doce fresco e as 3.3 kg restantes eram produtos de milho doce enlatado (USDA, 2010).

E pensando no consumo in-natura do milho algumas características são importantes para o processo de melhoramento como o número de grãos por espiga, o tamanho e largura das espigas que são indicadores chave para a avaliação da qualidade do milho (CAIRNS et al., 2013). Os métodos tradicionais para estimar essas características baseiam-se em observações manuais (MILLER et al., 2017), esses métodos são trabalhosos, demorados e pouco eficientes, muitas vezes sujeitos a erros.

A utilização de sistemas que utilização “machine vision” podem adquirir informações fenotípicas de uma maneira rápida e eficiente (VALIENTE-GONZÁLEZ et al, 2014). Este tipo de tecnologia está sendo cada vez mais utilizado na extração de informações de características de cereais (NARENDRA et al., 2010; MAKANZA et al., 2018), incluindo milho. Alguns trabalhos obterão as informações sobre as espigas como numero/grãos, número de fileiras, tamanho e largura, basicamente utilizando duas diferentes abordagens uma utilizando um mecanismo rotativo que captura imagens de toda a superfície da espiga (SONG et al., 2011), neste caso o sistema de rotação da espiga aumenta o custo e também torna este método de baixo rendimento e a segunda abordagem é a simples obtenção de uma única imagem da espiga (WU et al., 2020).

A qualidade da estimativa dos descritores de produtividade utilizando imagens depende de vários fatores, no entanto a utilização de apenas uma imagem é muito mais barato e pode ser adaptado para programas de melhoramento (WU et al., 2020; YAN et al., 2010; BELAN et al., 2018).

3 MATERIAL AND METHODS

3.1. Experiment

This study used 210 ears of sweet corn from the germplasm bank of the University of Florida. These ears came from a diverse population with wide genetic variability, introduced from different locations in the world (Figure 1). The experiment to obtain the phenotyped ears was carried out in the spring harvest, in 2019, at the “Everglades Research and Education Center” located in South Florida, in the city of Belle Glade (26° 41' 6.95" N de latitude and -80° 40' 16.59" W longitude).

Figure 1: Sweet corn ears that represent the studied population.

Source: Ricardo Andrade (2020).

The harvested ears were processed, husked and then taken to a dryer, for approximately 5 days, with an average temperature of 36°C, to moisture close to 13%.

3.2. Manual Evaluation

In the laboratory, ears were manually evaluated with the aid of a millimeter caliper for some traits directly related to grain yield and important visual requirements for the commercialization of fresh sweet corn. The descriptors measured were: length: obtained by the vertical distance from the base to the tip of the ear and width: obtained by the horizontal distance between the rows of grains at the midpoint of the ear. Additionally, traits such as number of grains and rows of a side of the ear, were determined by manual counting by viewing the images on a computer screen.

3.3. Obtaining digital images

After the phenotypic manual evaluation, digital images of the ears were captured using a professional Nikon D750 camera, equipped with a 35mm DX lens, with a built-in autofocus motor, 1.8f aperture and ISO setting (camera sensor's sensitivity to light) set to 1,200. Images were obtained in compression format JPG, RGB (red, green and blue) color system and resolution of 2,944 x 1,968 pixels.

In order for the images to be obtained with better quality, the camera was attached to a wooden structure, with three sides covered with white fabric, which avoided shading, and a base covered with black fabric, which provided greater background uniformity and contrast with the ears. No artificial light was used to obtain the images, only the natural incidence of light (Figure 2).

Figure 2: Cabin with attached camera that was used to capture the images.

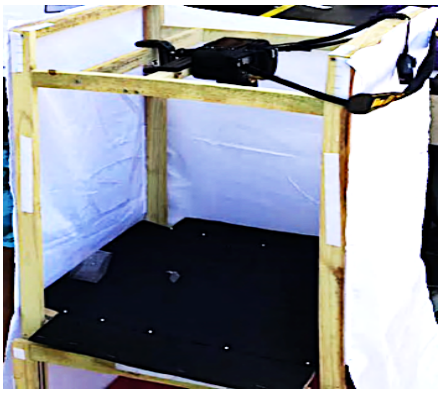

Source: Ricardo Andrade (2020).

3.4. Ear evaluation using digital images

C) Estimation of length and width of the ears

Images were processed with a view to standardizing the background, converting to a binary image and extracting the pixel matrix, in an automated way, aiming at phenotyping the ears in terms of length and width. For this, some steps were taken (Figure 3):

1- Loading the digital image in a Cartesian plane. The location of each pixel was represented by the perpendicular X and Y axes (Figure 3A);

2- Resizing the image to reduce the number of pixels and optimizing the computational process (Figure 3B);

3- Conversion of the image in the RGB color system (RED, GREEN, BLUE) to a gray scale (Figure 3C);

4 - Grayscale image thresholding. This process aims to segment the image into two groups based on the different gray level values (0 to 1). From the histogram of the grayscale image, a threshold of 50% was established (Figure 3D). Thus, all pixels with values above 0.5 were converted to 1 (white color) and all pixels below the threshold of 0.5 were set to 0 (black color), resulting in a binary image (0 and 1) (Figure 3E);

3- Finally, the pixels were uniformized and filled, eliminating noise present in the image and extracting the binary matrix (Figure 3F and 3G).

Figure 3: Image processing. A) Original image (dimension: 2,944 x 1,968); B) Image cut (dimension: 844 x 1,968); C) Gray scale; D) Gray-scale image histogram; E) Image thresholding; F) Elimination of image noise; G)Binary matrix

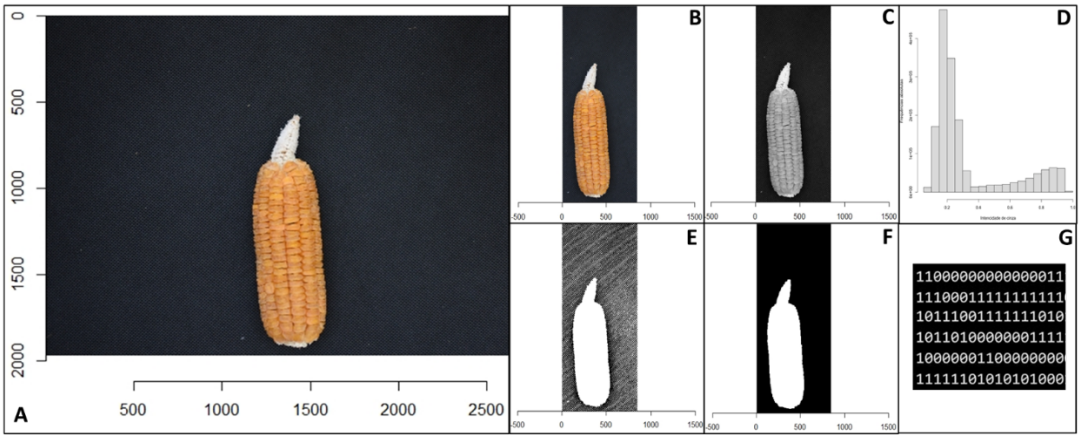

Source: Ricardo Andrade (2020).

The binary matrix generated after processing each image was used to obtain the length and width estimates in pixels. For that, only the elements equal to 1 that represented the ear area were extracted from the matrix. Subsequently, considering the Cartesian coordinates (x, y), the length of each ear (EA) was estimated by the following expression:

$$EA = \sqrt{(esp_a)^2 + (esp_d)^2},$$

where: esp_a corresponds to the difference between the maximum and minimum points on the Y axis. Considering only the maximum and minimum points of Y, there are many corresponding pixels on the X axis, so we obtained the average of the pixels in X for maximum Y and minimum Y. The estimate of esp_d corresponds to the difference between the average of the X pixels corresponding to the maximum Y and the average of the X pixels corresponding to the minimum Y. In this expression, esp_d was used to correct possible errors associated with ear slope. In cases where the ear did not show inclination, esp_d was considered equal to zero and the height was given by the difference between the maximum and minimum points on the Y axis (Figure 4).

Figure 4: Estimated height of ears in pixels. A) Ear height without slope, without correction. B) Ear height with inclination, with slope, calculated by the straight line perpendicular to the points of maximum Y and minimum Y.

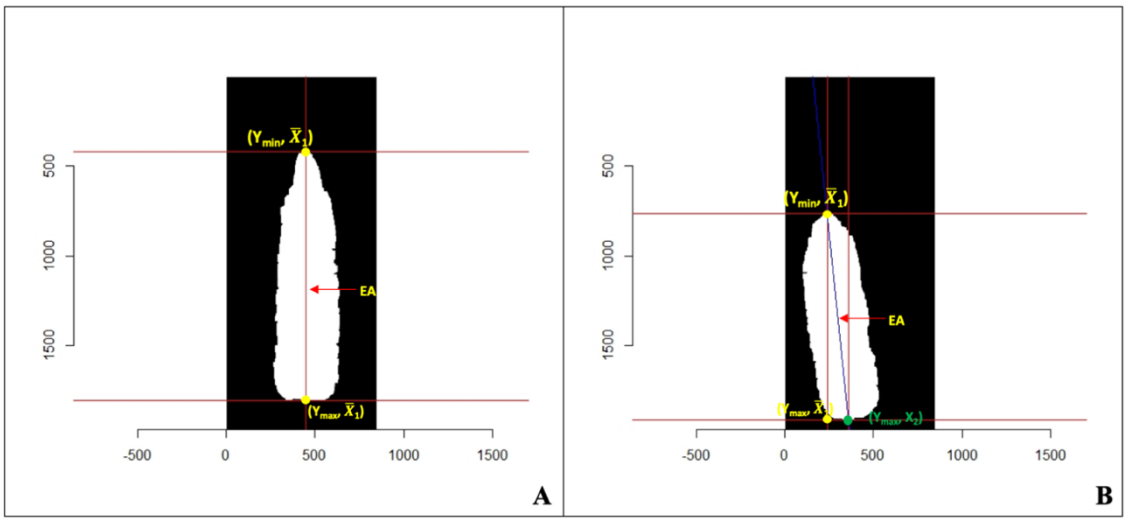

Source: Ricardo Andrade (2020).

The width estimate (EL) in pixels was given by the length of the straight line perpendicular to the height of each ear. To measure the ear width, it was previously necessary to find the value corresponding to the length midpoint on the Y axis and the angular coefficient of the perpendicular line (m), from the reduced equation of the line y $y = mx + c$, where x and y are the points belonging to the line and c is the linear coefficient that represents the numerical value through which the line passes through the ordinate (Y) axis. Thus, ear width was determined by the following expression:

$$EL = \sqrt{(adjacent\ side)^2 + (opposite\ side)^2},$$

where: adjacent side corresponds to the difference between the maximum pixel and the minimum pixel in X considering the length midpoint in Y; opposite side corresponds to the tangent of the angle m multiplied by the adjacent side. As for height, the value of the opposite side was used to correct possible errors associated with the slope of the ears (Figure 5).

Figure 5: Estimated pixel width. A) Ear width, without slope determined only by the estimate of the adjacent side; B) Ear width, with slope, determined by the equation presented above that takes into account the correction by the opposite side.

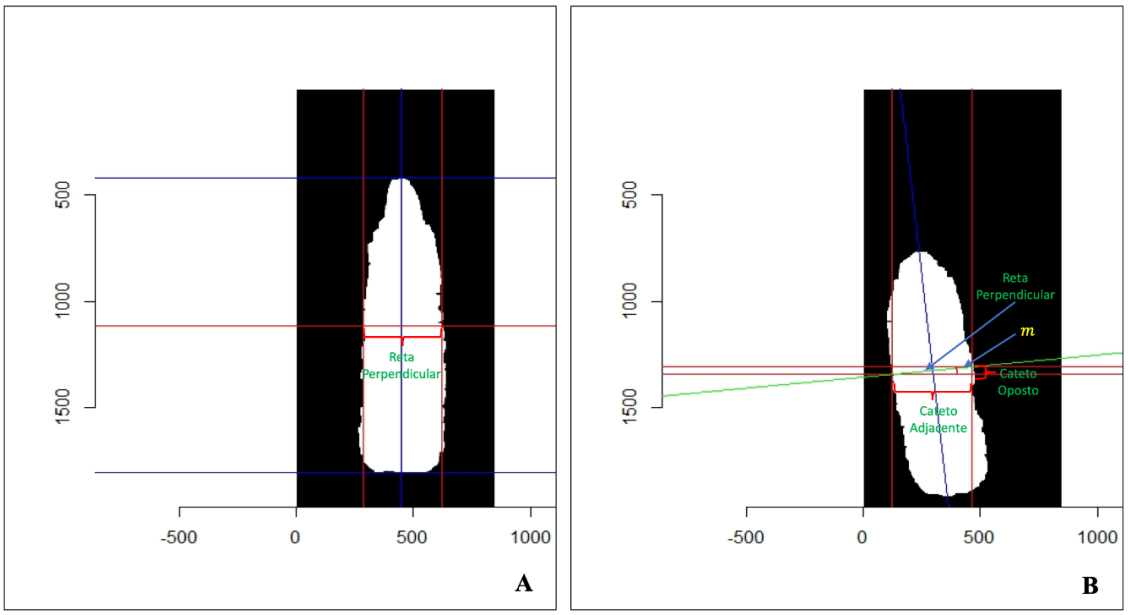

Source: Ricardo AndradeDo autor (2020).

B) Estimation of ear area (EA)

To isolate the representative area of the ear from the background, we used the image segmentation technique called K-nearest neighbors (KNN) proposed by Fukunaga and Narendra (1975). This technique consists of dividing the digital image into multiple regions or segments (set of pixels) that are similar, using a calculation algorithm that models the segmentation task in a semi-interactive manner. This study aimed to eliminate the background of the images and, therefore, it was necessary to provide the coordinates of the pixels that represented this region.

After identifying the area of interest, the image was converted from the RGB color system to a grayscale, consequently the image was segmented by means of thresholding, and later converted to a binary image. Thus, the pixels representing the ear were converted to a value of 1. They were used to estimate the proportionality of the ear area in relation to the total number of pixels observed in the image. To determine the ear area in square millimeters (mm), the number of pixels was converted to mm, with each 9.14 pixels corresponding to 1 mm.

C) Estimation of area without grain filling (ASEG)

Of the 212 ears that were phenotyped, 37 had a failure in grain filling. The determination of the ear area without grain filling followed the same steps performed to determine the total ear area, involving the thresholding techniques (50% threshold) and the KNN segmentation technique. By color difference, a representative point of ASEG was identified in each image. Subsequently, this portion was isolated, thresholded and converted to a binary matrix (Figure 6). From the binary pixel matrix, ASEG was estimated. To determine the proportion of ASEG in each ear, the ratio of ASEG to its total area was performed.

Figure 6: Estimation of area without grain filing using the KNN image segmentati technique.

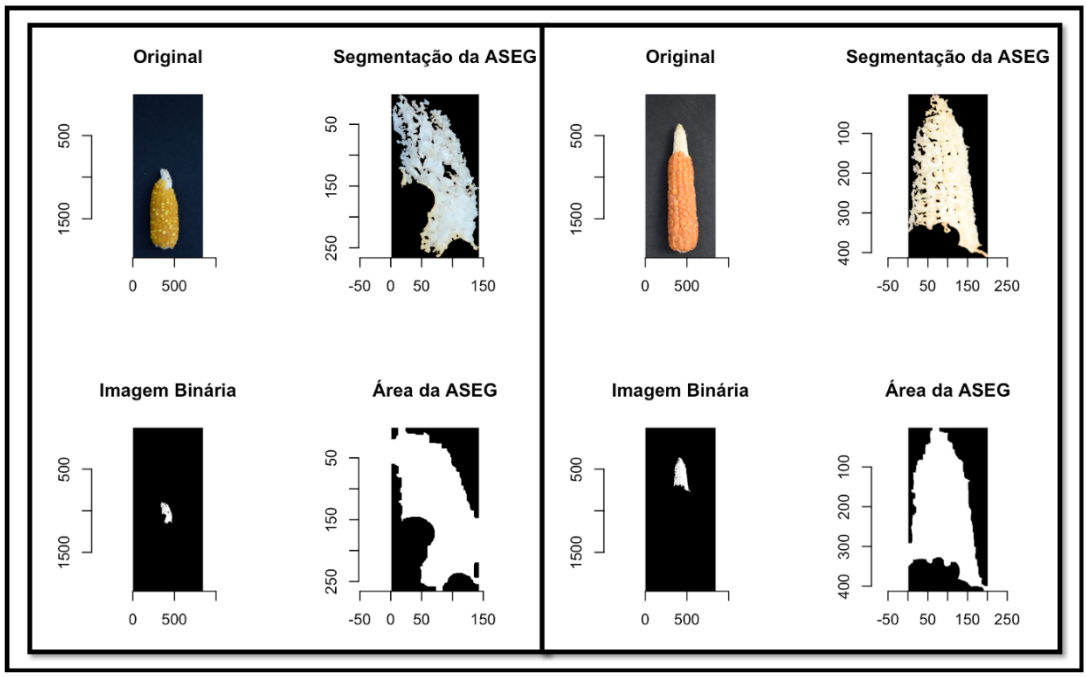

Source: Ricardo Andrade (2020).

D) Prediction of the number of grains

After processing the images, it was found that some of them were obtained with low quality in relation to focus, sharpness and color saturation. In addition, some ears did not have a well-defined number of rows and grains and are considered difficult to measure both manually and through image phenotyping. Therefore, a group of 91 images was selected.

In order to estimate the number of grains per ear, a reduction in the image size around the ear limits was previously performed, in order to proceed with a faster analysis. Subsequently, the following steps were followed:

1- Image rotation in case of ear slope. For this, a straight theta angle was determined based on the line between two points parallel to the ear length (Figure 7A).

2- Image segmentation based on the KNN technique. For that, an index that involves operations between RGB matrices was used, allowing the elimination of the image background. In the present study, the index used was the SHP (table 1). Subsequently a binary mask was created, which returned an image in shades of gray. Then, this grayscale image was interpreted as a topographic map, in which the limits between the hydrographic basins (segmentation) are considered the limits between the grains present in the ear (Matias et al., 2020) (Figure 7B).

3- Identification of the ear area, followed by counting the number of grains. For each ear, a new image was plotted with red dots on the grains that were identified (Figure 7C and 7 D).

Figure 7: Grain number count. A) Ear rotation; B) Image segmentation; C) Ear area identification; D) Number grain identification and count.

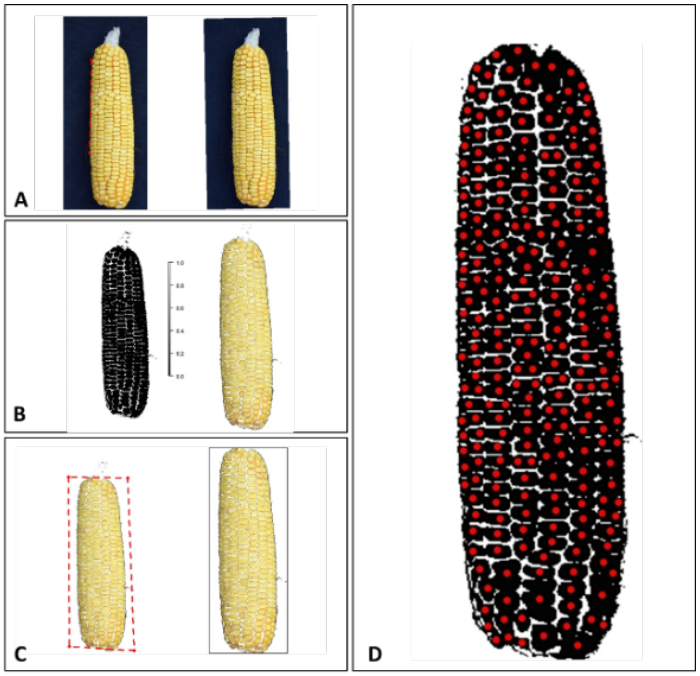

Source: Ricardo Andrade (2020).

E) Prediction of the number of rows

To predict the number of rows per ear, the same group of images selected was used to estimate the number of grains. Image processing for estimating the number of grains was based on the following criteria:

a. Resizing the image and extracting the matrix of pixels in the RGB channels. These matrices were used in a second moment to predict the number of rows (Figure 8).

b. Conversion of the image in the RGB color system (red, green, blue) to a gray scale and later to a binary image (0 and 1) or black and white;

c. Image segmentation using a 75% threshold and noise elimination.

Figure 8: Images from RGB matrices, used to predict the number of rows.

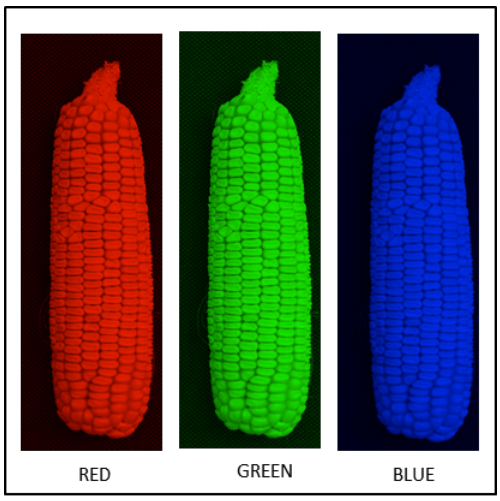

Source: Ricardo Andrade (2020).

1- Binary erosion: this technique allowed to eliminate sets of small pixels and/or to reduce areas of large sets of similar pixels. This technique allowed to individualize and quantify the grains and the rows of ears, when they were very close (Figure 9).

Figure 9: Segmentation techniques used A) Threshold 75% and B) Threshold 75% combined with the EROD technique, to identify the number of rows per ear.

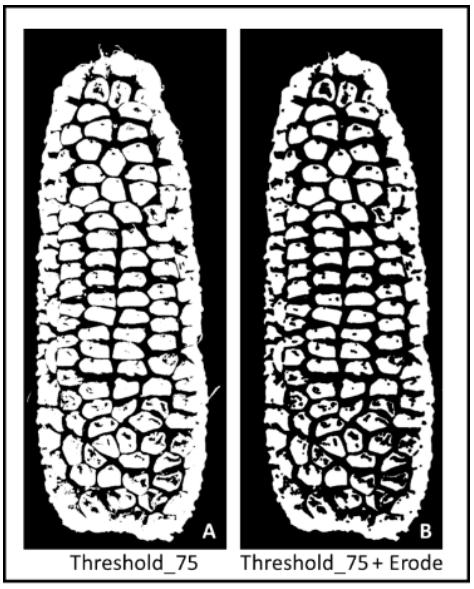

Source: Ricardo Andrade (2020).

To estimate the number of rows per ear, a prediction model was used. In addition, five different types of pixel matrices (red, green, blue, Threshold 75% (binary matrix) and Threshold 75% + EROD (binary matrix) were tested. The pixel matrix had an n x p dimension, where n is the number of images (or phenotyped ears) and p is the number of pixels of each image. The line of pixels that characterized each ear was obtained in two ways:

1) Line corresponding to the midpoint of each ear. The midpoint was obtained by the difference between the maximum pixel and the minimum pixel divided by two.

2) Average of 100 center pixels on each ear.

After obtaining the pixel matrix, the following prediction model was adopted:

$$\hat{\boldsymbol{y}} = \mathbf{X}\hat{\beta} + \mathbf{Z}\boldsymbol{\alpha} + \mathbf{e},$$

where $\hat{y}$ is the phenotypic value $n \times 1$ where $\boldsymbol{n}$ is the number of rows in each ear; $\boldsymbol{X}$ is the incidence matrix of the fixed effects vector ($\hat{\beta}$); $\boldsymbol{Z}$ is the incidence matrix of the ears; $\boldsymbol{\alpha}$ is the vector of pixels; **e** is the vector of residuals. Given the assumption of independence and normality for the random effects $\boldsymbol{\alpha}$ and **e**, we have: $\boldsymbol{\alpha} \sim N(0, \sigma_g^2 G)$, where G is the pixel matrix of the ears $\mathbf{e} \sim N(0, \sigma_r^2 R)$.

The predictive ability of the model was based on the results provided by the BGLR program, following the cross-validation technique. For this, images were randomly divided into five mutually exclusive groups, allowing the assessment of prediction skills under a 5-fold cross-validation scheme. The prediction quality measure was attributed based on the average performance of the five validations. The training population consisted of 73 images and the validation population was represented by 18 images. In each fold, 40,000 interactions were made, considering a burn-in of 10,000. The predictive ability of the model was verified by estimating the correlation between the predicted values and their corresponding phenotypic values evaluated manually.

3.5. Evaluation of the phenotyping efficiency

In order to check the phenotyping efficiency by means of digital images and its agreement with manual phenotyping, some reliability measures described in the literature were estimated for the traits length, width, number of rows and number of grains.

Reliability measures used:

a) slope (β) and coefficient of determination (R^2) of simple linear regression without i intercept (model: Y = βX + e, where Y is the value obtained from the image analysis, β is the slope and X the value obtained with manual measurement. The value of β was tested by the *t*-test, with $\alpha \leq 0.05$, whose hypotheses were: Ho: β = 1 and H1: β ≠ 1);

b) Bias (Bias = $\hat{\beta}$ – 1);

c) Person correlation (r) (Eq. 1), according to classification proposed by Hopkins (2000)

$$r = \frac{\sum_{i=1}^{n}(X_i - \bar{X}) * (Y_i - \bar{Y})}{\sqrt{\sum_{i=1}^{n}(X_i - \bar{X})^2} * \sqrt{\sum_{i=1}^{n}(Y_i - \bar{Y})^2}}$$

d) agreement index (d) proposed by Willmont *et al*. (1985);

$$d = 1 - \frac{\sum_{i=1}^{n}(X_i - Y_i)^2}{\sum_{i=1}^{n}(|Y_i - \bar{X}| + |X_i - \bar{X}|)^2}$$

e) performance index (c) proposed by Camargo; Sentelhas (1997);

$$c = r * d$$

f) Method efficiency (EF) proposed by Zacharias *et al*. (1996);

$$EF = \frac{\sum_{i=1}^{n}(X_i - \bar{X})^2 - \sum_{i=1}^{n}(X_i - Y_i)^2}{\sum_{i=1}^{n}(X_i - \bar{X})^2}$$

g) mean absolute error (MAE);

$$MAE = \frac{1}{n}\sum_{i=1}^{n}|Y_i - Y_i|$$

h) absolute maximum error (AMEX).

$$AMEX = MAX(|X_i - Y_i|)_{i=1}^{n}$$

Where X_i corresponds to the i-th value obtained with manual measurement, Y_i represents the i-th value observed from the image analysis, Y_i the average of the values obtained by manual measurement and $\bar{Y}$ the average of the values observed from the analysis of images.

All image processing and statistical analysis were performed using the softwares R (R DEVELOPMENT CORE TEAM, 2019) and GENES (CRUZ, 2013).

4 RESULTS AND DISCUSSION

In the present study, methods for phenotyping of corn ears were presented through the analysis of digital images using computational resources. All images were processed using segmentation techniques. Subsequently, matrices with information that helped to characterize the evaluated genotypes were extracted from the images (Figure 10). This process proved to be very efficient, in relation to the time spent when compared to manual evaluation. To measure length, width, number of rows and grains, it took approximately 30 hours of work and three evaluators. On the other hand, the computational process to estimate the same traits in all ears was performed by a single person in approximately 4 hours.

Figure 10: Automated processing for ear phenotyping using computational resources.

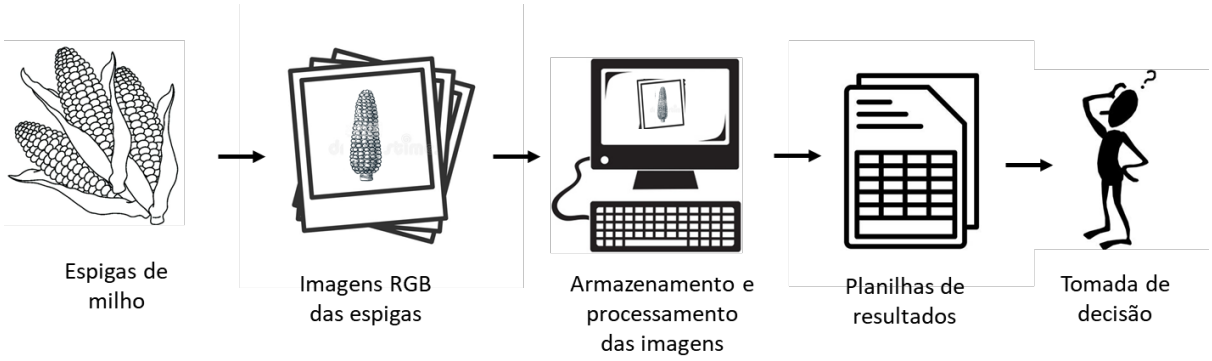

Source: Ricardo Andrade (2020).

Several studies found in the literature in recent years, also point out the advantages of adopting high yield phenotyping for traits of interest to the breeder, especially when phenotyping involves many individuals, resulting in an expensive and low precision process. The use of images in plant breeding programs has made the characterization of

individuals more efficient, reducing labor and time spent (MOREIRA et al., 2019; MAKANZA et al., 2018; MILLER et al., 2017; KOMYSHEV et al., 2017).

The 210 ears of sweet corn showed large phenotypic variation for all evaluated descriptors. This was indispensable to validate the proposed methodologies because different patterns of ears were tested. Ear length varied from 6.9 to 19.8 centimeters, while the width varied from 1.9 to 4.7 centimeters. The estimate of the regression coefficient (R^2) for length and width was approximately 0.88 for both traits, indicating a high association between the values obtained by manual phenotyping and the values extracted via image. On the other hand, when the slope of the line (β) was tested by the t-test, a significant difference of 1 ($\alpha \leq 0.05$) was found for both length and height, indicating the absence of a 1: 1 ratio between the values observed and estimated via image (Figure 11).

Figure 11: Scatter plot of the manual evaluations (x) versus (y) analysis by digital images for evaluating corn ears in terms of A) length and B) width.

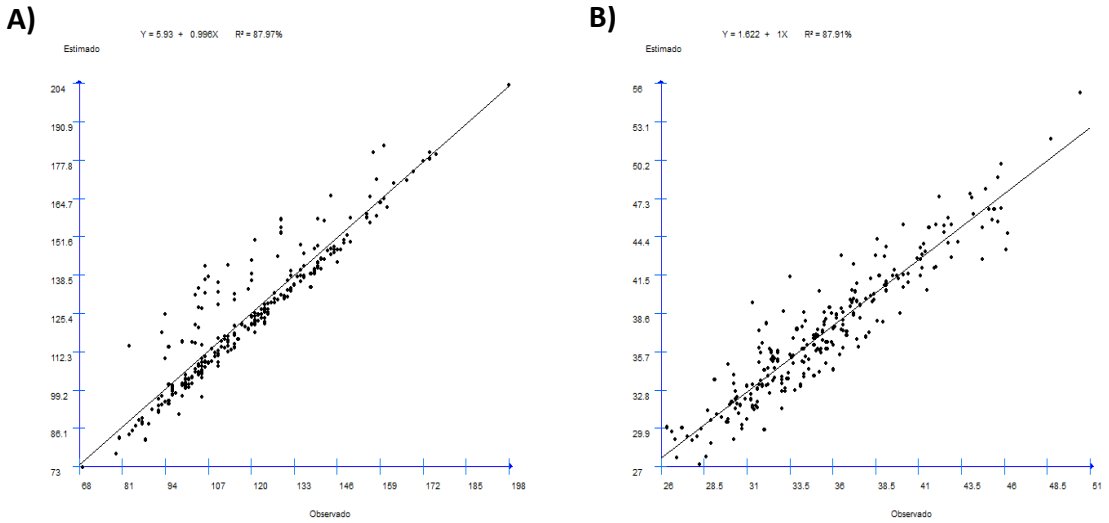

Source: Ricardo Andrade (2020).

From the results it is clear that manual phenotyping of ears for length and width, can be replaced by the characterization through images. The results observed in this study are consistent with those presented by Makanza et al. (2018). These authors verified correlation estimates above 0.9 for both traits and demonstrated that the length and width can be determined by the longest distance between two points along the longest and shortest axis of the ear.

The methodology proposed in this study for phenotyping the length and width of the ears, can also be extrapolated to infer grain yield. According to Greveniotis et al., (2019), both traits are directly correlated with productivity and, therefore, the variation in the length and width of the ears in different years and conditions, can provide information to the breeder on the productive performance of the genotypes evaluated. Despite this, it is important that these measures are associated with other descriptors as they are highly influenced by the effect of years, planting density and spacing between rows in the field.

The number of rows and grains per ear are also traits highly associated with yield and, therefore, there is a great interest on the part of researchers in obtaining these estimates. In spite of this, the information associated with these descriptors is usually obtained manually, requiring time and most of the time they are not accurate, because depending on the number and the arrangement of the grains on the ear, there may be a mistake by the evaluators at the time of counting.

To characterize the ears in terms of the number of grains and rows, only 91 images were used. Despite this, the phenotypic variation for these traits was also large, ranging from 66 to 188 for number of grains and from 10 to 18 for number of rows. To determine the number of grains per ears, several indices available in the literature were tested for image segmentation. The index that allowed for better isolation and consequently more accurate results in the grain count was the “Shape index” or SHP (Table 1).

For this descriptor, there was a variation between the number of grains determined by manual counting and by image processing of up to 99 grains more or less. In this case, the correlation between the observed and the estimated value was 0.59. Within this group of images, 40 images were verified with a maximum difference of 30 grains between the observed and estimated number, in these cases, the correlation was 0.95. When a maximum difference of 10 grains between the observed and estimated number was considered, 13 images were identified and the correlation value increased to 0.99.

The absence of a 1: 1 ratio between the observed and estimated values, for the number of grains considering the 91 images, was verified by the t-test ($\alpha \leq 0.05$) of the slope of the line (β). For this descriptor, the R^2 estimate was 0.35, showing a median association between the values obtained by manual phenotyping and those extracted by image processing (Figure 12).